

Rattling Behavior in a Simple Perovskite NaWO_3

Yuya Ikeuchi,[†] Hiroshi Takatsu,[†] Cédric Tassel,[†] **Craig M. Brown,[‡]** Taito Murakami,[†] Yuki Matsumoto,[†] Yoshihiko Okamoto,[§] and Hiroshi Kageyama^{*,†,‡}

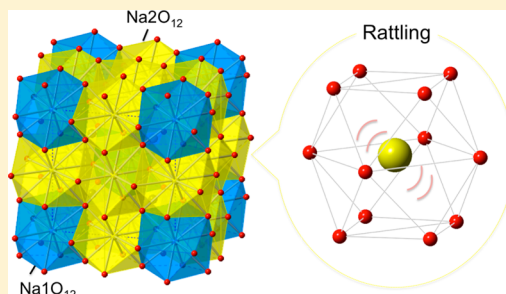
[†]Graduate School of Engineering, Kyoto University, Kyoto 615-8510, Japan

[‡]Center for Neutron Research National Institute of Standards and Technology Gaithersburg, Maryland 20899, United States

[§]Department of Applied Physics, Nagoya University, Nagoya 464-8603, Japan

Supporting Information

ABSTRACT: Rattling phenomena have been observed in materials characterized by a large cage structure but not in a simple ABO_3 -type perovskite because the size mismatch, if it exists, can be relieved by octahedral rotations. Here, we demonstrate that a stoichiometric perovskite oxide NaWO_3 , prepared under high pressure, exhibits anharmonic phonon modes associated with low-energy rattling vibrations, leading to suppressed thermal conductivity. The structural analysis and the comparison with the ideal perovskite KWO_3 without rattling behavior reveal that the presence of two crystallographic Na1 ($2a$) and Na2 ($6b$) sites in NaWO_3 (space group $Im\bar{3}$) accompanied by three in-phase WO_6 octahedral ($a^+a^+a^+$) rotations generates an open space $\Delta \sim 0.5 \text{ \AA}$ for the latter site, which is comparable with those of well-known cage compounds of clathrates and filled skutterudites. The observed rattling in NaWO_3 is distinct from a quadruple perovskite $\text{AA}'_3\text{B}_4\text{O}_{12}$ (A, A': transition metals) where the A ($2a$) site with lower multiplicity is the rattler. The present finding offers a general guide to induce rattling of atoms in pristine ABO_3 perovskites.



INTRODUCTION

Inorganic solids with a network of polyhedral cages that host guest cations show interesting properties associated with characteristic phonon modes.^{1–4} When guest cations are smaller relative to the space inside the cage, a local and anharmonic vibration, or “rattling”, occurs, leading to strong scattering of long wavelength acoustic phonons in clathrates (e.g., $\text{Sr}_8\text{Ga}_{16}\text{Ge}_{30}$),^{5,6} superconductivity with strong electron–phonon coupling in β -pyrochlore KOs_2O_6 ,^{7–9} and heavy Fermion states in filled skutterudites (e.g., $\text{SmOs}_4\text{Sb}_{12}$).^{10–13} It has been widely believed that the rattling vibration suppresses the lattice thermal conductivity, κ_L , resulting in the enhancement of thermoelectric efficiency.^{14–16} Quasi-harmonic interaction between the cage and guest cation is also proposed.¹⁷ These features have stimulated numerous studies toward exotic physical properties coupled with rattling vibrational modes, such as high efficiency thermoelectric materials with low κ_L .

Perovskite ABO_3 is the most studied system in materials science because of the richness in chemical and physical properties including superconductivity,¹⁸ colossal magnetoresistivity,¹⁹ and ferroelectricity.²⁰ The diversity of properties arises from the ability of perovskite compounds to take various cations at the A and B sites,²¹ along with the substitution of oxide site by other anions.²² In addition, octahedral rotation of various patterns causes the deviation of $\angle\text{B–O–B}$ angle from 180° in the ideal perovskite, which influences orbital overlap, superexchange interactions, and electron hopping between neighboring B sites. Here, the relief of size mismatch is the origin of octahedral rotations: when the Goldschmidt tolerance

factor is smaller than 1, BO_6 octahedra rotate to satisfy the necessary the A site cation environment, leading to structural distortion from a cubic perovskite (space group: $Pm\bar{3}m$).²¹ Octahedral rotations match almost any A site sizes, leading to dense structures and therefore leaving little “open space” for rattling to occur. Recently, Tanaka et al. reported several quadruple perovskite oxides, $\text{ACu}_3\text{V}_4\text{O}_{12}$ (A = Mn, Cu).^{23,24} In general, the A' ions in $\text{AA}'_3\text{B}_4\text{O}_{12}$ are Jahn–Teller active transition metals (e.g., Cu^{2+} and Mn^{3+}), and extensive BO_6 octahedral tilting permits square-planar $\text{A}'\text{O}_4$ coordination.²⁵ The resultant A site is 12-fold coordinated typically occupied by large alkaline earth metals (e.g., La), but when it is occupied by small transition metal ions, a rattling phenomenon emerges, as seen from a large atomic displacement parameter (ADP) and Einstein-like specific heat.^{23,24}

In this paper, we report the high-pressure synthesis of a stoichiometric tungsten bronze Na_xWO_3 ($x = 1$). Na_xWO_3 has been extensively studied for decades, and a perovskite structure with $a^+a^+a^+$ octahedral rotation (space group: $Im\bar{3}$) is found in a high concentration regime ($x \geq 0.8$).^{26–29} However, there remains an uncertainty about its Na composition, as will be shown later. The present study follows our recent work on K_xWO_3 , where the high-pressure method expanded the x amount, forming a stoichiometric tetragonal phase $\text{K}_{0.6}\text{WO}_3$ and a cubic (perovskite) one KWO_3 .³⁰ Quite unexpectedly, we observed rattling behavior in this *pristine* perovskite NaWO_3

Received: January 25, 2019

Published: April 29, 2019

but not in KWO_3 . We discuss the origin of the rattling phenomenon in NaWO_3 by considering crystal structures and physical properties, in comparison with the 1:3 ordered quadruple perovskite $\text{AA}'_3\text{B}_4\text{O}_{12}$. A general guideline to the rattling phenomenon in perovskite is presented.

EXPERIMENTAL PROCEDURE

Polycrystalline samples of Na_xWO_3 ($x = 0.5, 0.6, 0.75, 0.8, 1.0$) were prepared using a high-pressure (HP) technique. Stoichiometric mixtures of Na_2WO_4 , WO_2 (99%, Rare Metallic), and WO_3 (99.999%, Rare Metallic) were ground in a mortar for 30–60 min and pressed into a pellet. The pellets were sealed in a platinum capsule, inserted in a graphite tube heater, and enclosed in a pyrophyllite cube. These procedures were carried out in a N_2 -filled groove box. The Na_2WO_4 precursor was prepared by heating $\text{Na}_2\text{WO}_4 \cdot 2\text{H}_2\text{O}$ (99.8%, Alfa Aesar) in air at 400 °C for 24 h; a complete loss of water was checked by infrared spectroscopy.³¹ The HP reactions were performed at 1000 °C for 30 min under pressures of 5–8 GPa. The samples were characterized through powder X-ray diffraction (XRD) with $\text{Cu K}\alpha$ radiation at room temperature (RT). Synchrotron powder X-ray diffraction (SXRDXRD) measurements were performed at RT on the BL02B2 beamline at SPring-8. The wavelengths employed were $\lambda = 0.42044 \text{ \AA}$ for $x = 0.5, 0.6, 0.75, 1.0$ and $\lambda = 0.41914 \text{ \AA}$ for $x = 0.8$. A glass capillary with a 0.2 mm inner diameter was used. The SXRDXRD patterns were analyzed by the Rietveld refinement method using the program JANA2006.^{32,33} Reaction procedures were similar to those followed for the synthesis of $\text{Li}_{0.5}\text{WO}_3$, with stoichiometric mixtures of Li_2WO_4 (99%, Kojundo Chemical), WO_2 (99%, Rare Metallic), and WO_3 (99.999%, Rare Metallic). Neutron diffraction (ND) measurements ($\lambda = 1.5397 \text{ \AA}$) for $\text{Li}_{0.5}\text{WO}_3$ were carried out using the high-resolution powder diffractometer BT-1 at the NIST Center for Neutron Research. The sample was loaded into a vanadium cell. The collected neutron data were analyzed by the program JANA2006.

Specific heat, C_p , was measured with a commercial calorimeter (Quantum Design PPMS) in a temperature range from 200 to 2 K. Thermal conductivity, κ , was measured by a standard four-contact method at temperatures between 300 and 100 K. Electrical resistivity, ρ , was measured with a four-probe method using a commercial apparatus (Quantum Design PPMS) equipped with an adiabatic demagnetization refrigerator. We used rectangular-shaped samples cut out from the pellets. Gold wires were attached to the samples with silver paste. Magnetization was measured with a SQUID magnetometer (Quantum Design, MPMS).

RESULTS AND DISCUSSION

Figure 1a shows powder XRD patterns for a series of Na_xWO_3 at RT, which are indexed with a tetragonal supercell of a perovskite structure ($2a_p \times 2a_p \times 2c_p$) for $x \leq 0.75$ and a cubic supercell ($2a_p \times 2a_p \times 2a_p$) for $x \geq 0.8$, as indicated

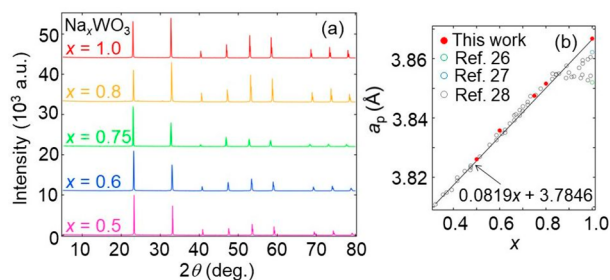


Figure 1. (a) Powder XRD patterns of Na_xWO_3 measured at RT. (b) Pseudocubic (normalized) lattice parameters, a_p , plotted as a function of x , where data from previous studies^{26–28} are included. The solid line represents the proposed relationship, $a_p(x) = 0.0819x + 3.7846$.

previously.^{28,29} No impurity phases were detected for all samples. In Figure 1b, we plotted the x dependence of the reduced cell parameters, a_p , along with those of previous reports, where the samples were prepared by solid-state reaction at ambient pressure.^{26–28} The results for $x \leq 0.8$ agree with the previous results. Whereas the reported data show a deviation from the Vegard law above $x = 0.85$, our samples follow a linear evolution in the entire range up to $x = 1$. Extrapolating the proposed relation, $a_p = 0.0819x + 3.7846$,²⁸ to $x = 1$ gives $a_p = 3.8665 \text{ \AA}$, which is fairly consistent with the experimental value of $3.86596(1) \text{ \AA}$. This fact strongly suggests that previous studies overestimated the Na content for $x > 0.85$. Deviation from the nominal values in earlier works may be due to Na evaporation. The use of high pressure prevented such undesirable evaporation. Higher compressibility of alkali metal may can also help Na ions be incorporated in the perovskite lattice.

A Rietveld refinement for the $x = 1$ data assuming the $\text{Im}\bar{3}$ structure confirmed the full stoichiometry of our specimen, with reasonable reliability factors of $R_{\text{wp}} = 7.37\%$ and $R_p = 5.70\%$ and goodness-of-fit of 2.22 (Figure 2a and Table 1).

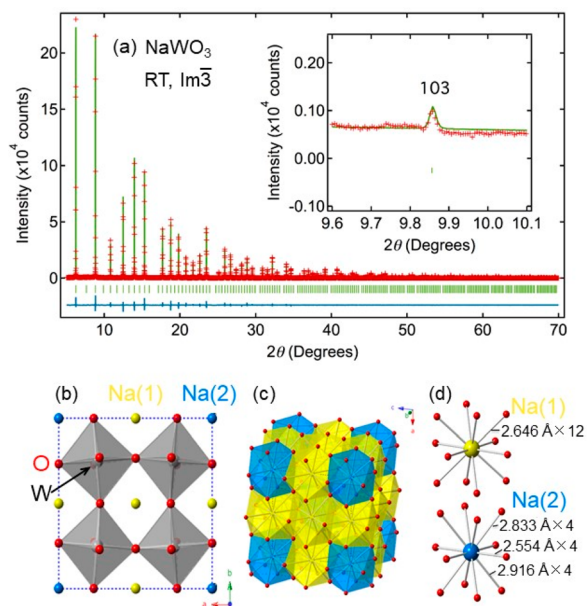


Figure 2. (a) Rietveld refinement of SXRDXRD of NaWO_3 at RT. Red crosses, green solid line, and blue solid line represent observed, calculated, and difference intensities, respectively. The green ticks are the position of Bragg peaks. The inset shows the (103) reflection. (b) Crystal structure of NaWO_3 ($\text{Im}\bar{3}$) with octahedral rotation of $a^+a^+a^+$. Blue, yellow, gray, and red spheres denote Na1 ($2a$), Na2 ($6b$), W ($8c$), and O ($24g$), respectively. The dotted lines show a $2a_p \times 2a_p \times 2a_p$ cell. (c) Two nonequivalent cubooctahedral units of NaO_{12} around Na1 (yellow) and Na2 (blue). (d) Coordination geometry around Na1 (top) and Na2 (bottom).

Table 1. Refined Structural Parameters of Na_xWO_3 ($x = 1.0$) at RT (Space Group: $\text{Im}\bar{3}$ (No. 204), $a = 7.731934(8) \text{ \AA}$)

atom	site	x	y	z	$U_{\text{iso}} (\times 10^{-2} \text{ \AA}^2)$
Na	$2a$	0	0	0	0.7(2)
Na	$6b$	0	1/2	1/2	2.23(15)
W	$8c$	1/4	1/4	1/4	0.238(2)
O	$24g$	0	0.263(2)	0.230(2)	0.77(7)

Rietveld analyses for other Na_xWO_3 samples gave results consistent with nominal Na compositions (Figure S1 and Table S1). It is remarkable that ADP of the Na2 site for NaWO_3 ($x = 1$) is $2.23(15) \times 10^{-2} \text{ \AA}^2$. This value corresponding to the isotropic root-mean-square displacement (rmsd) of $0.15(1) \text{ \AA}$ implies unusually large thermal vibration of sodium ions at the Na2 ($6b$) site. No anomaly is observed for the Na1 ($2a$) site ($\text{ADP} = 7 \times 10^{-3} \text{ \AA}^2$).

Together with our previous report,³⁰ we have two *isoelectric* (d^1) compounds, NaWO_3 ($Im\bar{3}$) with $a^+a^+a^+$ rotations and KWO_3 ($Pm\bar{3}m$) with $a^0a^0a^0$ rotations. This offers an ideal opportunity to clarify the effect of WO_6 octahedral rotation on physical properties. First, let us present the temperature variation of resistivity, ρ , and magnetic susceptibility, χ ($=M/H$), in Figure 3. Both compounds exhibit metallic temperature

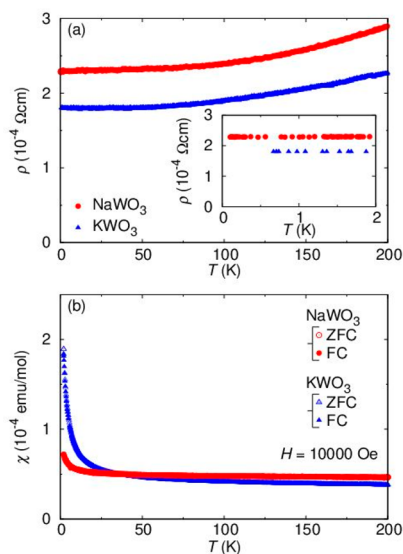


Figure 3. (a) Temperature dependence of electrical resistivity, ρ , for $0.1 \text{ K} < T < 200 \text{ K}$ in NaWO_3 and $0.6 \text{ K} < T < 200 \text{ K}$ in KWO_3 . The low- T region is magnified in the inset. (b) Temperature dependence of magnetic susceptibility, χ , for NaWO_3 and KWO_3 in the zero-field- and field-cooling process.

dependence and almost the same ρ values in a whole temperature range examined (Figure 3a), where no signature of phase transition is observed. This behavior is paralleled with T -independent χ (Figure 3b), and hence, both compounds can be attributed to a Pauli paramagnetic metal. The Curie-type increases in χ at low temperatures below 20 K come from a small amount of free impurity spins (0.01 – 0.1%).

On the contrary, heat capacities of the two compounds behave differently, as shown in Figure 4a (C_p/T versus T). This difference can be highlighted for the C_p/T^3 – T plot (Figure 4b). A broad peak is observed at 30 K only for NaWO_3 , suggesting the presence of a low-energy optical phonon. A similar peak in the C_p/T^3 versus T curve has been known to appear in cage compounds having large ADPs:^{9,34,35} these two features, namely, C_p/T^3 peak and large ADPs, are hallmarks of local vibrational mode (or rattling) associated with guest cations inside cages.^{3,4} Thus, the observed broad peak of NaWO_3 is most likely attributed to Na2 ($6b$) ions with the large ADP.

The C_p/T^3 peak of cage compounds is typically characterized by Einstein specific heat within the “harmonic” approximation.^{9,34,35} To do this, we analyzed our raw data of

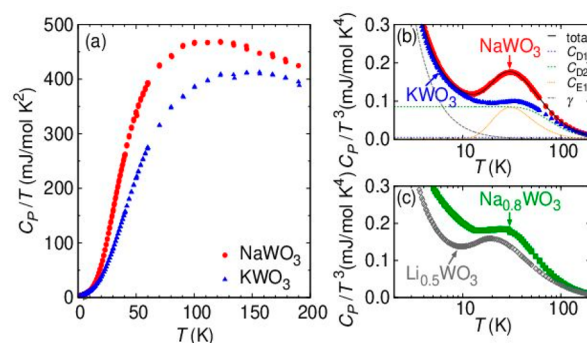


Figure 4. (a) Temperature dependence of (a) C_p/T and (b) C_p/T^3 for NaWO_3 and KWO_3 . Lines are fitting results (see the text for detail). (c) C_p/T^3 versus T plot for $\text{Na}_{0.8}\text{WO}_3$ and $\text{Li}_{0.5}\text{WO}_3$.

NaWO_3 by a combination of Debye and Einstein specific heats, along with an electronic specific heat of $C_e(T) = \gamma T$ (where γ is the electronic specific heat constant), which is given by

$$C_p(T) = \sum_i f_{D,i} C_{D,i}(T) + \sum_j f_{E,j} C_{E,j}(T) + C_e(T) \quad (1)$$

where $f_{D,i}$ and $f_{E,j}$ represent the number of the Debye and Einstein modes for the i th and j th contributions, respectively, all of which were determined by fitting. The sum of these is nothing but the total number of phonon modes in the unit cell, that is, $\sum_i f_{D,i} + \sum_j f_{E,j} = 15$. $C_{D,i}(T)$ and $C_{E,j}(T)$ denote, respectively, Debye and Einstein specific heat, which are expressed as follows:

$$C_{D,i}(T) = 3R \left(\frac{T}{\Theta_{D,i}} \right)^3 \int_0^{\Theta_{D,i}/T} \frac{e^x x^4 dx}{(e^x - 1)^2} \quad (2)$$

$$C_{E,j}(T) = R \frac{e^{\Theta_{E,j}/T}}{(e^{\Theta_{E,j}/T} - 1)^2} \left(\frac{\Theta_{E,j}}{T} \right)^2 \quad (3)$$

Here, R is the gas constant and $\Theta_{D,i}$ and $\Theta_{E,j}$ are Debye and Einstein temperatures, respectively, that were also used as fitting parameters. The least-squares fitting was carried out using the data in the temperature range of $2 \text{ K} < T < 200 \text{ K}$. A reasonable agreement was obtained for NaWO_3 when we assume two Debye and one Einstein modes ($i = 2, j = 1$) and for KWO_3 with two Debye modes only ($i = 2, j = 0$) (see Figure 4b and Table 2). It is clear that the additional Einstein term can reproduce the main feature of the C_p/T^3 peak in NaWO_3 , suggesting rattling-like local vibrational mode. It is noteworthy that the introduction of Na site deficiency (i.e., $\text{Na}_{0.8}\text{WO}_3$) substantially suppresses the C_p/T^3 peak, as shown in Figure 4c. This implies that the effect of lattice defect and disorder is not the origin of the peak, as opposed to random or

Table 2. Parameters Obtained by Fitting the Specific Heat Data of NaWO_3 to Equation 1, Where a Model with Two Debye and One Einstein Mode Was Used^a

mode	$\Theta_{D,i}$ $\Theta_{E,j}$ (K)	$f_{D,i}$ $f_{E,j}$
D_1	962	6.62
D_2	371	6.74
E_1	151	1.64

^aThe terms of the Debye and Einstein modes are D_i ($i = 1, 2$) and E_1 . The γ value was obtained as $\gamma = 3.34 \text{ mJ/K}^2$.

disordered systems such as those containing Bi or Pb with 6s lone pair electrons.^{36,37}

The observed rattling phenomenon in NaWO₃ is unprecedented because the simple ABO₃ perovskite can be described by cubic closed-packed arrangement of AO₃ layers with B cations occupied at the interstitial octahedral site, and if the A cation is smaller, BO₆ octahedral rotation takes place to adjust and optimize the local coordination environment around A. In NaWO₃, however, the a⁺a⁺a⁺ rotation generates nonequivalent Na sites, Na1 (2a) and Na2 (6b) (Figure 2b,c). This necessarily leads to a situation that both sites cannot be simultaneously optimized in terms of the local environment, yielding relatively large guest-free-space Δ around the Na2 ion. The value of Δ can be roughly estimated by taking the difference between the cage distance d_{cage} (from the center) and ionic radius of a guest cation: $\Delta = d_{\text{cage}} - r(\text{Na}^+)$. Our structural analysis indicates that Na1 has 12 equidistant Na1–O bonds (2.701(18) Å), whereas Na2 has four short (2.552(17) Å), four medium (2.778(17) Å), and four long (2.916(17) Å) bonds (Figure 2d). The available space of Na1 and Na2 is estimated by calculating $d_{\text{cage}} = d - r(\text{O}^{2-})$,^{9,24,34,35,38} where d is the Na–O bond length and $r(\text{O}^{2-})$ refers to the ionic radius of O²⁻ (=1.4 Å).³⁹ This yielded $d_{\text{cage}} = 1.301$ Å for Na1 and 1.152, 1.378, and 1.516 Å for Na2. Subsequently, using $r(\text{Na}^+) \sim 1$ Å,³³ we obtained $\Delta \sim 0.3$ Å for Na1O₁₂ and $\Delta \sim 0.5$ Å for Na2O₁₂. The Δ value of Na2O₁₂ is parallel with those in the known cage compounds: $\Delta = 0.5$ – 0.9 Å for filled skutterudites,^{35,38} $\Delta = 0.3$ – 0.4 Å for A-site-ordered quadruple perovskites,^{23,24} and $\Delta = 1$ – 3 Å for clathrates and β -pyrochlores.^{3,4,9,34} Together with the large rmsd of 0.15 Å, the large value of Δ for Na2 led us to conclude that the Na2 site is responsible for rattling local vibration.

A comparison with the A-site-ordered quadruple perovskite CuCu₃V₄O₁₂ further revealed that the coefficient of the Einstein specific heat, $f_{E,1} = 1.64$ per the NaWO₃ formula, is larger than 0.27 per the “CuVO₃” formula (i.e., $1/4 \times \text{CuCu}_3\text{V}_4\text{O}_{12}$).^{24,33} This result is fairly consistent with the difference in the rattling site: CuCu₃V₄O₁₂ has a rattler at the A site (2a) with the 2-fold multiplicity, whereas NaWO₃ has a rattler at the A' site (6b) with 6-fold multiplicity. Another prominent feature that differentiates NaWO₃ from CuCu₃V₄O₁₂ is the degree of octahedral tilting. Although both compounds are isostructural, the octahedral (a⁺a⁺a⁺) tilting in CuCu₃V₄O₁₂ is very extensive and gives the $\angle\text{V–O–V}$ bridging angle of $\sim 140^\circ$, which forces the A' site transition metal to adopt the square-planar coordination. As a result, the A site can be a rattler. In contrast, the $\angle\text{W–O–W}$ angle for NaWO₃ is $\sim 169^\circ$, meaning that moderate octahedral rotation makes the A' site a rattler.

One can generalize a strategy to find rattling phenomena in the pristine ABO₃ perovskite. Among 15 tilting systems in perovskite,^{26,40–42} four systems (a⁺a⁺a⁺, a⁰b⁺b⁺, a⁰b⁺c⁻, and a⁰a⁺c⁻) have nonequivalent A sites. Examples include Li_xWO₃ ($x \leq 0.5$) and Li_{0.2}ReO₃ with a⁺a⁺a⁺,⁴³ NaTaO₃, NaNbO₃, SrZrO₃, and SrHfO₃ with a⁰b⁺c⁻,^{41,44} and NH₄MnCl₃ with a⁰b⁺c⁻.⁴¹ Unfortunately, most of them exist as an intermediate phase (e.g., 803–893 K for NaTaO₃). As far as we are aware, Li_{0.5}WO₃ with a⁺a⁺a⁺ is stable at RT,³³ so we prepared the phase-pure Li_{0.5}WO₃ under high pressure and measured C_p . As expected, a C_p/T^3 peak is found at 20 K, which can be fitted by introducing the Einstein specific heat with $\Theta_E = 98$ K (Figure 4c and Figure S4 and Table S4). Extensive research on rattling compounds has shown that Θ_E decreases with increasing the

cage size.^{3,4,34,35,38} In fact, the smaller Θ_E value for Li_{0.5}WO₃ (versus 151 K for NaWO₃) could be related to a larger Δ value of ~ 1 Å.

In order to see the effect of rattling on physical properties, we measured κ for NaWO₃, the result of which is plotted in Figure 5, together with the data for KWO₃. The κ for NaWO₃

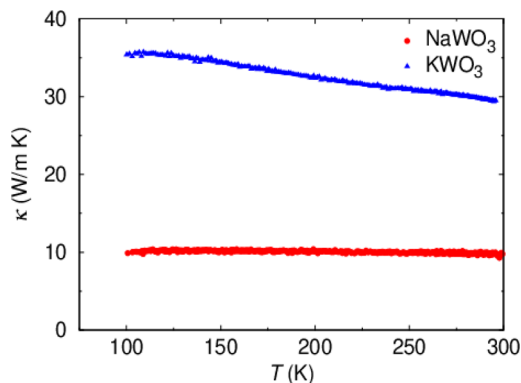


Figure 5. Temperature dependence of thermal conductivity κ of NaWO₃ and KWO₃.

is clearly larger than that for KWO₃ in the whole temperature range measured. The Wiedemann–Franz law was used to extract the electronic contribution of thermal conductivity κ_e . Using the 200 K data of ρ , we obtained $\kappa_e = 1.6$ W/m·K for NaWO₃ and $\kappa_e = 2.2$ W/m·K for KWO₃. Hence, the difference in κ is ascribed to that of lattice thermal conductivity, κ_L , but is different from what can be expected from the weight difference of K⁺ and Na⁺ ions.^{45,46} We thus conclude that rattling vibration of Na⁺ ions largely suppresses κ_L for NaWO₃. The suppression of κ_L is discussed for cage compounds in the context of the rattling effect.^{13–15,46} More recently, the rattling and its relation with the suppression of κ_L are discussed in compounds without cage structure^{47,48} such as LaOBiS_{2–x}Se_x, where rattling-like local vibration is found in a cation at the planar coordination geometry with lone pair electrons. These findings give us hope to explore compounds beyond well-known cage systems toward finding low κ_L .

CONCLUSION

We have extended the solubility limit of Na_xWO₃ to the full stoichiometry ($x = 1$) by exploiting a high-pressure route. NaWO₃ crystallizes in a perovskite structure with all in-phase octahedral rotations (a⁺a⁺a⁺). Despite the pristine perovskite phase, the specific heat measurement on NaWO₃ exhibits anharmonic phonon modes associated with low-energy rattling vibrations, which is absent in the ideal cubic perovskite KWO₃. The rattling behavior in NaWO₃ is caused by the presence of distinct crystallographic Na sites. The structural analysis revealed that the Na2 (6b) site is a rattler, as opposed to the isostructural quadruple AA₃B₄O₁₂ perovskite, where the rattling site is the A (2a) cation. The present finding suggests that rattling phenomenon will be available for other ABO₃ perovskites with nonequivalent A sites. Conversely, a cation order may be possible by introducing different alkali metals (e.g., A = Na, A' = K) in this structural type. Together with our recent study on stoichiometric phases of K_{0.6}WO₃ and KWO₃,²⁹ the high-pressure method turned out to be highly efficient: Li_xWO₃ ($0.5 \leq x \leq 1$) in the LiNbO₃ structure is also isolated.

■ ASSOCIATED CONTENT

S Supporting Information

The Supporting Information is available free of charge on the ACS Publications website at DOI: 10.1021/acs.inorgchem.9b00248.

Detailed information on sample preparation, measurements of physical properties (electrical resistivity, specific heat, and thermal conductivity), and analysis of specific heat (PDF)

Accession Codes

CCDC 1893481 contains the supplementary crystallographic data for this paper. These data can be obtained free of charge via www.ccdc.cam.ac.uk/data_request/cif, or by emailing data_request@ccdc.cam.ac.uk, or by contacting The Cambridge Crystallographic Data Centre, 12 Union Road, Cambridge CB2 1EZ, UK; fax: +44 1223 336033.

■ AUTHOR INFORMATION

Corresponding Author

*E-mail: kage@scl.kyoto-u.ac.jp.

ORCID

Hiroshi Kageyama: 0000-0002-3911-9864

Notes

The authors declare no competing financial interest.

■ ACKNOWLEDGMENTS

Synchrotron and neutron experiments were performed at SPring-8 BL02B2 of JASRI and BT-1 of the NIST Center for Neutron Research. We thank Dr. K. Fujita for giving us heat capacity data of $\text{CuCu}_3\text{V}_4\text{O}_{12}$. The work was supported by CREST (JPMJCR1421) and JSPS KAKENHI (JP16H6439, 17H04849).

■ REFERENCES

- (1) Nolas, G. S.; Morelli, D. T.; Tritt, T. M. SKUTTERUDITES: A Phonon-Glass-Electron Crystal Approach to Advanced Thermoelectric Energy Conversion Applications. *Annu. Rev. Mater. Sci.* **1999**, *29*, 89–115.
- (2) Sato, H.; Sugawara, H.; Aoki, Y.; Harima, H. *Handbook of Magnetic Materials*; Elsevier: Amsterdam, 2009; Vol. 18, Chapter 1, p 1.
- (3) Takabatake, T.; Suekuni, K.; Nakayama, T.; Kaneshita, E. Phonon-glass Electron-crystal Thermoelectric Clathrates: Experiments and Theory. *Rev. Mod. Phys.* **2014**, *86*, 669–716.
- (4) Hiroi, Z.; Yamaura, J.; Hattori, K. Rattling Good Superconductor: β -Pyrochlore Oxides AOs_2O_6 . *J. Phys. Soc. Jpn.* **2012**, *81*, 011012.
- (5) Nolas, G. S.; Cohn, J. L.; Slack, G. A.; Schujman, S. B. Semiconducting Ge Clathrates: Promising Candidates for Thermoelectric Applications. *Appl. Phys. Lett.* **1998**, *73*, 178–180.
- (6) Nolas, G. S.; Poon, J.; Kanatzidis, M. Recent Developments in Bulk Thermoelectric Materials. *MRS Bull.* **2006**, *31*, 199–205.
- (7) Yonezawa, S.; Muraoka, Y.; Matsushita, Y.; Hiroi, Z. Superconductivity in a Pyrochlore-related Oxide KO_2O_6 . *J. Phys. J. Phys.: Condens. Matter* **2004**, *16*, L9–L12.
- (8) Brühwiler, M.; Kazakov, S. M.; Karpinski, J.; Batlogg, B. Mass Enhancement, Correlations, and Strong-Coupling Superconductivity in the β -Pyrochlore KO_2O_6 . *Phys. Rev. B: Condens. Matter Mater. Phys.* **2006**, *73*, 094518.
- (9) Hiroi, Z.; Yonezawa, S.; Nagao, Y.; Yamaura, J. Extremely Strong-coupling Superconductivity and Anomalous Lattice Properties in the β -Pyrochlore Oxide KO_2O_6 . *Phys. Rev. B: Condens. Matter Mater. Phys.* **2007**, *76*, 014523.
- (10) Sanada, S.; Aoki, Y.; Aoki, H.; Tsuchiya, A.; Kikuchi, D.; Sugawara, H.; Sato, H. Exotic Heavy-Fermion State in Filled Skutterudite $\text{SmOs}_4\text{Sb}_{12}$. *J. Phys. Soc. Jpn.* **2005**, *74*, 246–249.
- (11) Hattori, K.; Hirayama, Y.; Miyake, K. ILocal Heavy Quasiparticle in Four-Level Kondo Model. *J. Phys. Soc. Jpn.* **2005**, *74*, 3306–3313.
- (12) Hotta, T. Effect of Rattling Phonons on Sommerfeld Constant. *J. Phys. Soc. Jpn.* **2008**, *77*, 103711.
- (13) Hotta, T. Inverse Isotope Effect on Kondo Temperature in Electron-Rattling System. *J. Phys. Soc. Jpn.* **2009**, *78*, 073707.
- (14) Nolas, G. S.; Slack, G. A.; Morelli, D. T.; Tritt, T. M.; Ehrlich, A. C. The effect of Rare-earth Filling on the Lattice Thermal Conductivity of Skutterudites. *J. Appl. Phys.* **1996**, *79*, 4002–4008.
- (15) Sales, B. C.; Mandrus, D.; Williams, R. K. Filled Skutterudite Antimonides: A New Class of Thermoelectric Materials. *Science* **1996**, *272*, 1325–1328.
- (16) Keppens, V.; Mandrus, D.; Sales, B. C.; Chakoumakos, B. C.; Dai, P.; Coldea, R.; Maple, M. B.; Gajewski, D. A.; Freeman, E. J.; Bennington, S. Localized Vibrational Modes in Metallic Solids. *Nature* **1998**, *395*, 876–878.
- (17) Koza, M. M.; Johnson, M. R.; Viennois, R.; Mutka, H.; Girard, L.; Ravot, D. Breakdown of Phonon Glass Paradigm in La- and Ce-filled $\text{Fe}_4\text{Sb}_{12}$ Skutterudites. *Nat. Mater.* **2008**, *7*, 805–810.
- (18) Sleight, A. W.; Gillson, J. L.; Bierstedt, P. E. High-temperature superconductivity in the $\text{BaPb}_{1-x}\text{Bi}_x\text{O}_3$ systems. *Solid State Commun.* **1975**, *17*, 27–28.
- (19) Kuwahara, H.; Tomioka, Y.; Asamitsu, A.; Moritomo, Y.; Tokura, Y. A First-Order Phase Transition Induced by a Magnetic Field. *Science* **1995**, *270*, 961–963.
- (20) Megaw, H. D. Origin of ferroelectricity in barium titanate and other perovskite-type crystals. *Acta Crystallogr.* **1952**, *5*, 739–749.
- (21) Tilley, R. J. D. *Perovskites: Structure–Property Relationships*; John Wiley & Sons, Ltd.: Chichester, UK, 2016.
- (22) Kageyama, H.; Hayashi, K.; Maeda, K.; Atfield, J. P.; Hiroi, Z.; Rondinelli, J. M.; Poeppelmeier, K. R. Expanding frontiers in materials chemistry and physics with multiple anions. *Nat. Commun.* **2018**, *9*, 772.
- (23) Akizuki, Y.; Yamada, I.; Fujita, K.; Nishiyama, N.; Irifune, T.; Yajima, T.; Kageyama, H.; Tanaka, K. A-Site-Ordered Perovskite $\text{MnCu}_3\text{V}_4\text{O}_{12}$ with a 12-Coordinated Manganese(II). *Inorg. Chem.* **2013**, *52*, 11538–11543.
- (24) Akizuki, Y.; Yamada, I.; Fujita, K.; Taga, K.; Kawakami, T.; Mizumaki, M.; Tanaka, K. Rattling in the Quadruple Perovskite $\text{CuCu}_3\text{V}_4\text{O}_{12}$. *Angew. Chem., Int. Ed.* **2015**, *54*, 10870–10874.
- (25) Shimakawa, Y. A-Site-Ordered Perovskites with Intriguing Physical Properties. *Inorg. Chem.* **2008**, *47*, 8562–8570.
- (26) Straumanis, M. E. The Sodium Tungsten Bronzes. I, Chemical Properties and Structure. *J. Am. Chem. Soc.* **1949**, *71*, 679–683.
- (27) Brimm, E. O.; Brantley, J. C.; Lorenz, J. H.; Jellinek, M. H. Sodium and Potassium Tungsten Bronzes. *J. Am. Chem. Soc.* **1951**, *73*, 5427–5432.
- (28) Brown, B. W.; Banks, E. The Sodium Tungsten Bronzes. *J. Am. Chem. Soc.* **1954**, *76*, 963–966.
- (29) Clarke, R. New Sequence of Structural Phase Transitions in Na_xWO_3 . *Phys. Rev. Lett.* **1977**, *39*, 1550–1553.
- (30) Ikeuchi, Y.; Takatsu, H.; Tassel, C.; Goto, Y.; Murakami, T.; Kageyama, H. High-Pressure Synthesis of Fully Occupied Tetragonal and Cubic Tungsten Bronze Oxides. *Angew. Chem., Int. Ed.* **2017**, *56*, 5770–5773.
- (31) Fortes, A. D. Crystal Structures of Spinel-Type Na_2MoO_4 and Na_2WO_4 Revisited using Neutron Powder Diffraction. *Acta Cryst. E* **2015**, *71*, S92–S96.
- (32) Petříček, V.; Dušek, M.; Palatinus, L. Crystallographic Computing System JANA2006: General Features. *Z. Kristallogr. - Cryst. Mater.* **2014**, *229*, 345–352.
- (33) See the Supporting Information for powder XRD and SXRD data of Na_xWO_3 , the detailed structure analysis, and the analysis of the specific heat of Na_xWO_3 , Li_xWO_3 , and KWO_3 .

(34) Suekuni, K.; Avila, M. A.; Umeo, K.; Fukuoka, H.; Yamanaka, S.; Nakagawa, T.; Takabatake, T. Simultaneous Structure and Carrier Tuning of Dimorphic Clathrate $\text{Ba}_8\text{Ga}_{16}\text{Sn}_{30}$. *Phys. Rev. B: Condens. Matter Mater. Phys.* **2008**, *77*, 235119.

(35) Matsuhira, K.; Sekine, C.; Wakeshima, M.; Hinatsu, Y.; Namiki, T.; Takeda, K.; Shirotani, I.; Sugawara, H.; Kikuchi, D.; Sato, H. Systematic Study of Lattice Specific Heat of Filled Skutterudites. *J. Phys. Soc. Jpn.* **2009**, *78*, 124601.

(36) Melot, B. C.; Tackett, R.; O'Brien, J.; Hector, A. L.; Lawes, G.; Seshadri, R.; Ramirez, A. P. Large Low-temperature Specific Heat in Pyrochlore $\text{Bi}_2\text{Ti}_2\text{O}_7$. *Phys. Rev. B: Condens. Matter Mater. Phys.* **2009**, *79*, 224111.

(37) Takatsu, H.; Hernandez, O.; Yoshimune, W.; Prestipino, C.; Yamamoto, T.; Tassel, C.; Kobayashi, Y.; Batuk, D.; Shibata, Y.; Abakumov, A. M.; Brown, C. M.; Kageyama, H. Cubic Lead Perovskite PbMoO_3 with Anomalous Metallic Behavior. *Phys. Rev. B: Condens. Matter Mater. Phys.* **2017**, *95*, 155105.

(38) Yamaura, J.; Hiroi, Z. Rattling Vibrations Observed by Means of Single-Crystal X-ray Diffraction in the Filled Skutterudite $\text{RO}_4\text{Sb}_{12}$ ($R = \text{La}, \text{Ce}, \text{Pr}, \text{Nd}, \text{Sm}$). *J. Phys. Soc. Jpn.* **2011**, *80*, 054601.

(39) Shannon, R. D. Revised Effective Ionic Radii and Systematic Studies of Interatomic Distances in Halides and Chalcogenides. *Acta Crystallogr., Sect. A: Cryst. Phys., Diffr., Theor. Gen. Crystallogr.* **1976**, *32*, 751–767.

(40) Woodward, P. M. Octahedral Tilting in Perovskites. I. Structure Stabilizing Forces. *Acta Crystallogr., Sect. B: Struct. Sci.* **1997**, *53*, 32–43.

(41) Woodward, P. M. Octahedral Tilting in Perovskites. II. Structure Stabilizing Forces. *Acta Crystallogr., Sect. B: Struct. Sci.* **1997**, *53*, 44–66.

(42) Howard, C. J.; Stokes, H. T. Group-Theoretical Analysis of Octahedral Tilting in Perovskites. *Acta Crystallogr., Sect. B: Struct. Sci.* **1998**, *54*, 782.

(43) Cava, R. J.; Santoro, A.; Murphy, D. W.; Zahurak, S. M.; Roth, R. S. The Structures of the Lithium Inserted Metal Oxides $\text{Li}_{0.2}\text{ReO}_3$ and $\text{Li}_{0.36}\text{WO}_3$. *J. Solid State Chem.* **1983**, *50*, 121–128.

(44) Kennedy, B. J.; Howard, C. J.; Chakoumakos, B. C. High-Temperature Phase Transitions in SrHfO_3 . *Phys. Rev. B: Condens. Matter Mater. Phys.* **1999**, *60*, 2972–2975.

(45) Tritt, T. M. *Thermal Conductivity: Theory, Properties, and Applications*; Springer Science & Business Media: New York, 2005.

(46) Rowe, D. M. *CRC Handbook of Thermoelectrics*; CRC Press: Boca Raton, FL, 1995.

(47) Suekuni, K.; Lee, C. H.; Tanaka, H. I.; Nishibori, E.; Nakamura, A.; Kasai, H.; Mori, H.; Usui, H.; Ochi, M.; Hasegawa, T.; Nakamura, M.; Ohira-Kawamura, S.; Kikuchi, T.; Kaneko, K.; Nishiate, H.; Hashikuni, K.; Kosaka, Y.; Kuroki, K.; Takabatake, T. Retreat from Stress: Rattling in a Planar Coordination. *Adv. Mater.* **2018**, *30*, 1706230.

(48) Lee, C. H.; Nishida, A.; Hasegawa, T.; Nishiate, H.; Kunioka, H.; Ohira-Kawamura, S.; Nakamura, M.; Nakajima, K.; Mizuguchi, Y. Effect of Rattling Motion without Cage Structure on Lattice Thermal Conductivity in $\text{LaOBiS}_{2-x}\text{Se}_x$. *Appl. Phys. Lett.* **2018**, *112*, 023903.